Available online at www.sciencedirect.com
ScienceDirect
Journal of Sound and Vibration 299 (2007) 757–773
JOURNAL OF SOUND AND VIBRATION
www.elsevier.com/locate/jsvi

Vibration control of a tall building subjected to earthquake excitation

An-Pei Wang*, Yung-Hing Lin

Department of Civil Engineering, Chung-Yuan Christian University, Chung-Li, Taiwan 32023, ROC

Received 17 February 2004; received in revised form 4 March 2004; accepted 10 July 2006
Available online 10 October 2006

Abstract

The purpose of this paper is to develop two kinds of controllers: (1) the variable structure control (VSC) and (2) the fuzzy sliding mode control (FSMC), for the building with an active-tuned-mass damper (ATMD) structural control system. It is desired that the controlled system remain stable and effective when the building is subjected to from earthquake excitation. From simulation results, it is found that (1) the VSC and the FSMC methods successfully control vibrations of the building system under earthquake-induced excitation, (2) the FSMC method is more economical and practical than the VSC due to the smaller controlling force and associated control energy required.

1. Introduction

In the last three decades, controlling devices, passive as well as active, have been developed to suppress structural vibrations from environmental disturbances. Tuned-mass dampers (TMDs) are widely used to control vibrations in civil engineering structures that are subjected to earthquake-induced vibrations. To reduce excessive vibrations, passive mass dampers have been installed [1]. Although, TMDs are effective in reducing vibrations caused by stationary excitation forces, their performance to suppress seismic response are relatively limited [2]. The idea of active control for civil engineering structures started to emerge around 1970 [3]. An active-TMD (ATMD) has to be considered when the required resisting force exceeds the capacity of a passive-tuned-mass damper [2].

The variable structure control (VSC) principle can be adapted for the linear, stable and unstable systems [4,5]. However, The VSC theory cannot be directly applied to the ATMD control system since the motion equation of the control system is not of canonical form. In this paper, the control system is first transformed into a canonical form so that the sliding hyper-plane can be designed, and the VSC is used to control the ATMD system.

The theory of fuzzy sets established by *Zadeh* [6] has been extensively researched in various fields of engineering. For example, the clean water procedure of running water, the subway revolve, the car settle soon,

*Corresponding author. Fax: +886 3 2654299.
E-mail address: anpei@cycu.edu.tw (A.-P. Wang).

0022-460X/$ - see front matter © 2006 Elsevier Ltd. All rights reserved.
doi:10.1016/j.jsv.2006.07.016

the stock certificate invest and analyze, the medical treatment diagnostician and the control system with electric power. In control engineering, fuzzy theories were applied to the automatic control in stream engine by *Mamdani* [7]. The civil engineering community was also forthcoming in studying the application of the fuzzy theories and fuzzy controls [8,9]. The sliding mode and fuzzy control have been combined by Hwang et al. [10] to offer the application of pneumatic servo system in the fuzzy sliding mode control (FSMC) method.

In this paper, the building system is regarded as a distributed parameter system instead of a discrete lumped parameter system, which was investigated in the previous studies [11–13]. The dynamic equation of a building associated with the Active-tuned-mass-damper (ATMD) has been addressed by Wang et al. [14]. In this paper, the VSC and the FSMC methods are proposed to control vibrations of the building by control force in the ATMD. Runge–Kutta method is employed to obtain the numerical simulations associated with the application of the control laws. Finally, numerical results are compared and conclusions are drawn for the building with the ATMD structure control system. Although, the VSC has been quite extensively researched for structured control, this paper presented the formulation for converting the state-space representation of a multi-story building with ATMD at the roof to a canonical form for application of the VSC and the FSMC. It is found that the VSC and the FSMC methods successfully control vibrations of the building system under the earthquake, and the FSMC method is more economical and practical than the VSC due to the smaller controlling force.

2. Formulation of building with TMD

2.1. System description

A schematic drawing of the building with a TMD system is shown in Fig. 1(a). The fixed (OXY) and the moving coordinate ($o'xy$) are used to describe the whole system. The building is subjected to the earthquake motion $b(t)$. The building consists of n floors and has the concentrated mass m_i for the ith floor. The TMD is composed of a concentrated mass M_G, a spring with constant k, and an oil-hydraulic system, which generates force F acting on the building. When the contact surface between two solids is dry, Coulomb damping can be used to describe the friction force opposing their relative motion and its magnitude is denoted by $\mu M_G g$, in which μ is the so-called kinetic coefficient of friction. The building is modeled by Euler–Bernoulli beam theory with length L, mass density ρ, cross-sectional area A, elastic modules E and moment of inertia I. The positions of slabs are located at x_i $(i = 1, 2, \ldots, n)$. The transverse deflection $v(x, t)$ measured from the moving coordinate is a function of both spatial coordinate x and time t. In Fig. 1(b), the equilibrium position ξ of the mass M_G is measured from the nth slab. It is assumed that the distance between the concentrated mass M_G and rooftop is negligible compared to the building height L. The free-body diagram is shown in Fig. 1(c).

We obtain a set of nonlinear, second-order ordinary differential equations. The dynamic formulation has been addressed by Wang et al. [14] and detailed in Appendix.

$$\mathbf{M}\ddot{\mathbf{Q}} + \mathbf{K}\mathbf{Q} + \mathbf{N}(\mathbf{Q}) = \mathbf{P}, \tag{1}$$

where $\mathbf{M}$ and $\mathbf{K}$ are the global mass and stiffness matrices, $\mathbf{N}(\mathbf{Q})$ represents the nonlinear term, and $\mathbf{P}$ is the force vector. It should be noted that the force vector $\mathbf{P}$ includes the acceleration $\ddot{b}$ of earthquake, actuating force F and dry friction force $\mu M_G g \operatorname{sgn}(\dot{\xi})$.

Rayleigh damping is assumed to model the natural damping in the structure:

$$\mathbf{C} = \alpha\mathbf{M} + \beta\mathbf{K}, \tag{2}$$

where the coefficients α and β are selected to fit the structure under consideration.

Thus, we obtain the equation of motion for the damped system

$$\mathbf{M}\ddot{\mathbf{Q}} + \mathbf{C}\dot{\mathbf{Q}} + \mathbf{K}\mathbf{Q} + \mathbf{N}(\mathbf{Q}) = \mathbf{P}. \tag{3}$$

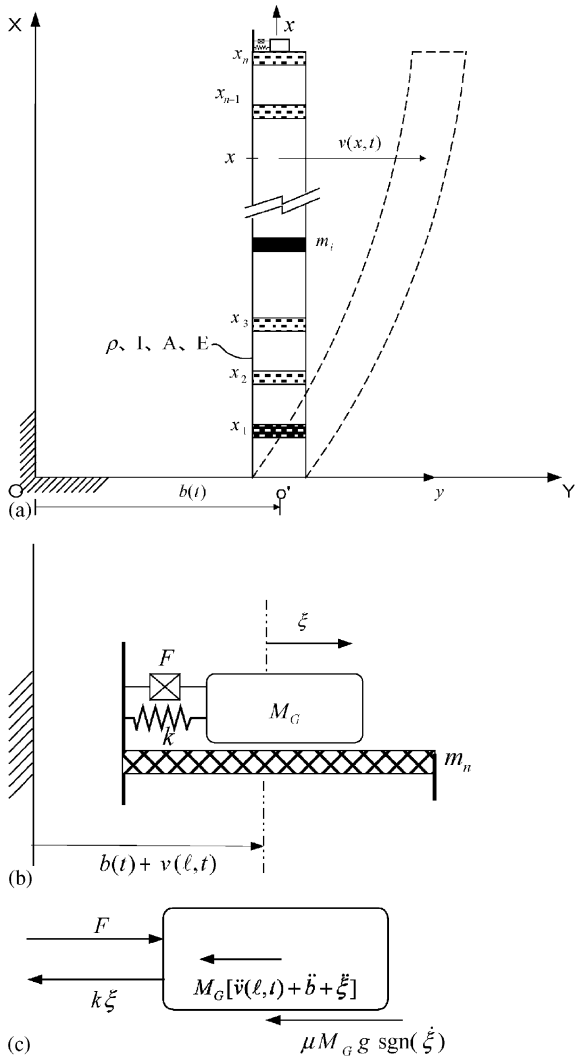

Fig. 1. (a) Schematic drawing of a building with the TMD system, (b) schematic diagram of a tuned-mass damper and (c) free-body diagram of the mass damper.

3. Control design

3.1. Variable structure control

The VSC [4,5] is often used to control the nonlinear and time-invariant systems due to its advantages of fast response, robustness, and good performance. The control design involves the determination of a sliding plane $s(x) = 0$ in the state space and makes the state trajectories hit and slide on it. The control design is divided into two stages. The first stage is the hitting condition or reaching mode, which describes the trajectory starting from initial state toward the sliding plane. In this stage, the hitting condition $s \cdot \dot{s} < 0$ is satisfied. The second stage is the sliding condition or sliding mode, in which the trajectory moves to the original of the phase plane. The characteristic root of $s(x) = 0$ must have negative value, thus the *Routh–Hurwitz* stability criterion is satisfied.

Since the actuating force directly acts on the ATMD structural control system, and the distributed building system has vibrations, the whole system is therefore a class of single-input multi-output (SIMO) system and is

rewritten as

$$\dot{\mathbf{Z}}(t) = \mathbf{A}\mathbf{Z}(t) + \mathbf{B}u(t) + \mathbf{W}(\mathbf{Z}, t),$$
$$\mathbf{Y}(t) = \mathbf{C}\mathbf{Z}(t), \tag{4}$$

where $\mathbf{A}$ is a $2n \times 2n$ system matrix, $\mathbf{B}$ is a $2n \times 1$ actuator position matrix, $\mathbf{C}$ is an $\mathbf{m} \times 2\mathbf{n}$ output matrix, $\mathbf{Z}(t)$ is a $2n \times 1$ state variable vector, $n = 2N_e + 1$, $u(t) = F(t)$ is the control input, $\mathbf{Y}(t)$ is an output variable vector, and $\mathbf{W}(\mathbf{Z}, t)$ is a disturbance vector and includes the nonlinear term, acceleration of earthquake and dry friction force. The detailed coefficients can be seen in Appendix.

Let the sliding plane be

$$s(t) = \mathbf{C} \cdot \mathbf{E}(t) = 0, \tag{5}$$

where $\mathbf{E}(t)$ is the error state vector, and $\mathbf{C} = [c_1, c_2, \ldots, c_{2n}]$ is its coefficient. For the purpose of vibration suppression, we have $\mathbf{E}(t) = -\mathbf{Z}(t)$.

The system (5) is linear, time-invariant but not a canonical controllable plant. The control system must be transformed to the canonical controllable form in which the VSC can be directly applied. The upper bound of disturbance vector, $\mathbf{W}(\mathbf{Z}, t)$, is omitted in the design of controllers, because the upper bound can be assumed a constant. System (5) is first transformed by $\bar{\mathbf{Z}}(t) = \mathbf{T}_1\mathbf{Z}(t)$ with $\mathbf{T}_1$ being an invertible transformation matrix and having $\mathbf{T}_1\mathbf{B} = \begin{bmatrix} \mathbf{O} \\ 1 \end{bmatrix}$, we have

$$\dot{\overline{\mathbf{Z}}}(t) = \overline{\mathbf{A}\mathbf{Z}}(t) + \bar{\mathbf{b}}u(t), \tag{6}$$

where

$$\overline{\mathbf{A}} = \mathbf{T}_1\mathbf{A}\mathbf{T}_1^{-1} = \begin{bmatrix} \overline{\mathbf{A}_{11}} & \overline{\mathbf{A}_{12}} \\ \overline{\mathbf{A}_{21}} & \overline{\mathbf{A}_{22}} \end{bmatrix}, \quad \bar{\mathbf{b}} = \mathbf{T}_1\mathbf{B} = \begin{bmatrix} \mathbf{O} \\ 1 \end{bmatrix}, \quad \overline{\mathbf{Z}}(t) = \begin{bmatrix} \overline{\mathbf{Z}_1}(t) \\ \overline{\mathbf{Z}_2}(t) \end{bmatrix}.$$

Eq. (6) can be written as

$$\dot{\overline{\mathbf{Z}_1}}(t) = \overline{\mathbf{A}_{11}\mathbf{Z}_1}(t) + \overline{\mathbf{A}_{11}\mathbf{Z}_2}(t), \tag{7a}$$

$$\dot{\overline{\mathbf{Z}_2}}(t) = \overline{\mathbf{A}_{21}\mathbf{Z}_1}(t) + \overline{\mathbf{A}_{22}\mathbf{Z}_2}(t) + u(t), \tag{7b}$$

where , $\overline{\mathbf{A}_{11}}$, $\overline{\mathbf{A}_{12}}$, $\overline{\mathbf{A}_{21}}$, and $\overline{\mathbf{A}_{22}}$ are the constant matrices, $\overline{\mathbf{Z}_1}(t)$ and $\overline{\mathbf{Z}_2}(t)$ are the state variable matrices, and $u(t)$ is the input force function.

The eigenfunction of $\overline{\mathbf{A}_{11}}(t)$ can be expressed as

$$p(\lambda) = \lambda^{2n-1} + a_{2n-1}\lambda^{n-2} + \cdots + a_2\lambda + a_1 = 0. \tag{8}$$

The dynamic system represented by Eq. (7) is further transformed by

$$\overline{\mathbf{Z}_1}(t) = \mathbf{T}_2\overline{\overline{\mathbf{Z}_1}}(t), \tag{9}$$

where

$$\mathbf{T}_2 = \begin{bmatrix} \overline{\mathbf{A}_{12}} & \overline{\mathbf{A}_{11}}\,\overline{\mathbf{A}_{12}} & \cdots & \overline{\mathbf{A}_{11}}^{2n-2}\overline{\mathbf{A}_{12}} \end{bmatrix} \begin{bmatrix} a_2 & a_3 & \cdots & a_{2n-1} & 1 \\ a_3 & a_4 & \cdots & 1 & 0 \\ \vdots & \vdots & \iddots & \vdots & \vdots \\ a_{2n-1} & 1 & 0 & \cdots & 0 \\ 1 & 0 & 0 & \cdots & 0 \end{bmatrix}.$$

By using transformation (9), Eq. (7a) becomes a controllable canonic form as follows:

$$\dot{\overline{\overline{\mathbf{Z}_1}}}(t) = \overline{\overline{\mathbf{A}_{11}\mathbf{Z}_1}}(t) + \overline{\overline{\mathbf{A}_{12}\mathbf{Z}_2}}(t), \tag{10}$$

where

$$\overline{\overline{\mathbf{A}_{11}}} = \mathbf{T}_2^{-1}\overline{\mathbf{A}_{11}}\mathbf{T}_2 = \begin{bmatrix} 0 & 1 & \dots & 0 & 0 \\ 0 & 0 & \dots & 0 & 0 \\ \vdots & \vdots & \vdots & \vdots & \vdots \\ 0 & 0 & \dots & 0 & 1 \\ -a_1 & -a_2 & \dots & -a_{2n-2} & -a_{2n-1} \end{bmatrix}, \quad \overline{\overline{\mathbf{A}_{12}}} = \mathbf{T}_2^{-1}\overline{\mathbf{A}_{12}} = \begin{bmatrix} 0 \\ 0 \\ \vdots \\ 0 \\ 1 \end{bmatrix}.$$

The state variable $\overline{\mathbf{Z}_2}(t)$ is assigned as

$$\overline{\mathbf{Z}_2}(t) = -\Delta\mathbf{a}^{\mathrm{T}}\overline{\overline{\mathbf{Z}_1}}(t) = -\Delta\mathbf{a}^{\mathrm{T}}\mathbf{T}_2^{-1}\overline{\mathbf{Z}_1}(t), \tag{11}$$

where

$$\Delta\mathbf{a}^{\mathrm{T}} = \begin{bmatrix} \bar{a}_1 - a_1 & \bar{a}_2 - a_2 & \dots & \bar{a}_{2n-2} - a_{2n-2} & \bar{a}_{2n-1} - a_{2n-1} \end{bmatrix},$$

in which $\bar{a}_1, \bar{a}_2, \dots, \bar{a}_{2n-1}$ depend on the designed poles of the switching function. Substituting Eq. (11) into Eq. (10),

$$\dot{\overline{\overline{\mathbf{Z}_1}}} = \left(\overline{\overline{\mathbf{A}_{11}}} - \overline{\overline{\mathbf{A}_{12}}}\Delta\mathbf{a}^{\mathrm{T}}\right)\overline{\overline{\mathbf{Z}_1}}(t), \tag{12}$$

The characteristic equation of the matrix $\left(\overline{\overline{\mathbf{A}_{11}}} - \overline{\overline{\mathbf{A}_{12}}}\Delta\mathbf{a}^{\mathrm{T}}\right)$ becomes

$$\lambda^{2n-1} + \bar{a}_{2n-1}\lambda^{2n-2} + \cdots + \bar{a}_2\lambda + \bar{a}_1 = 0. \tag{13}$$

In the above equation, we can assign the stable poles of the system according to the sliding plane:

$$s(t) = (D + r)^{2n-1}\mathbf{E}(t) = (D + r)^{2n-1}\mathbf{Z}(t) = 0, \tag{14}$$

where $D = \mathrm{d}/\mathrm{d}t$ and

$$\begin{aligned} \bar{a}_{2n-1} &= (2n-1)r, \\ &\vdots \\ \bar{a}_2 &= (2n-1)r^{2n-2}, \\ \bar{a}_1 &= r^{2n-1}. \end{aligned}$$

If we choose $r > 0$, Eq. (13) will satisfy Routh–Hurwitz stability condition. From Eq. (11), the designed sliding hyperplane is

$$\begin{aligned} s(t) &= \begin{bmatrix} -\Delta\mathbf{a}^{\mathrm{T}}\mathbf{T}_2^{-1} & 1 \end{bmatrix}, \\ \begin{bmatrix} \overline{\mathbf{Z}_1}(t) \\ \overline{\mathbf{Z}_2}(t) \end{bmatrix} &= \begin{bmatrix} -\Delta\mathbf{a}^{\mathrm{T}}\mathbf{T}_2^{-1} & 1 \end{bmatrix}, \\ \mathbf{T}_1\mathbf{Z}(t) &= \mathbf{C}\mathbf{E}(t), \end{aligned} \tag{15}$$

where $\mathbf{C} = \begin{bmatrix} -\Delta\mathbf{a}^{\mathrm{T}}\mathbf{T}_2^{-1} & 1 \end{bmatrix}\mathbf{T}_1$. On the sliding hyperplane, one obtains

$$s(t) = \mathbf{C} \cdot \mathbf{E}(t) = 0, \tag{16}$$

The VSC method needs the measurements of s and $\dot{s}$ in the control process. s is measured and obtained from the dynamic response. Consequently, it can be used to obtain

$$\dot{s}(t) = \frac{\mathrm{d}s(t)}{\mathrm{d}t} = \lim_{\Delta t \to 0} \frac{s(t + t_s) - s(t)}{t_s}, \tag{17}$$

where t_s is the time interval in simulation.

For the eventual sliding mode-switching scheme, the control is designed to satisfy Lyapunov stability criteria.

$$V = s^{\mathrm{T}}s > 0,$$
$$\dot{V} = \frac{\mathrm{d}}{\mathrm{d}t}(s^{\mathrm{T}}s) = 2s^{\mathrm{T}}\dot{s} = 2s^{\mathrm{T}}\frac{\partial s}{\partial Z}(AZ + Bu) < 0, \tag{18}$$

Here, the VSC for the control function $u(t)$ takes the form of relay. The relay gain maybe either fixed or state dependent [4]. The control function is

$$u(t) = \begin{cases} u^{+}, & \text{if } s > 0, \\ u^{-}, & \text{if } s < 0, \end{cases} \tag{19}$$

where the values u^{+} and u^{-} are chosen to satisfy the reaching condition. For example, we can selected $u^{+} = K$ and $u^{-} = -K$, where K depends on the upper bounded of the disturbances, $\mathbf{W}(\mathbf{Z}, t)$.

3.2. Fuzzy sliding mode control

The FSMC method is one of the control methods combining the fuzzy theory with sliding mode control method. It has a two-fold advantage: the fuzzy control handles the nonlinear control systems, and the sliding mode control offers a fast and stable control system. The FSMC diagram is shown in Fig. 2. It can be seen that the system includes two parts, one is the controller and structure, the other is the fuzzy sliding mode controller, which contains the observation, sliding plane and fuzzy controller.

Applying the traditional fuzzy *Mamdani* method [7] to the non-canonical control form (4) causes an improper control force and increases instability of the building system. In this paper, we first transfer the system to a canonical form the same as the VSC, then define the sliding plane $s(t) = 0$ and establish the switching function s of Eq. (15) and $\dot{s}$ of Eq. (17) to construct the FSMC method. First, we normalize s and $\dot{s}$ to S and $\dot{S}$ by $S = GS \cdot s$ and $\dot{S} = GCS \cdot \dot{s}$, where GS and GCS are determined by experience. Then, we change S and $\dot{S}$ to fuzzy variables, and take advantage of fuzzy control theory to design the control function U.

In this paper, the S, $\dot{S}$ and U are divided into 13 ranks of $\{-1, -5/6, -4/6, -3/6, -2/6, -1/6, 0, 1/6, 2/6, 3/6, 4/6, 5/6, 1\}$, seven fuzzy variables are defined as Positive Big [PB], Positive Medium [PM], Positive Small [PS], Zero [ZO], Negative Small [NS], Negative Medium [NM], and Negative Big [NB], and as shown in Fig. 3. The linguistic rules of S and $\dot{S}$ are set up in Table 1. In order to set up the look-up table, for two example rules to explain:

Rule 1: If S is PB and $\dot{S}$ is PB, then U is PB. Its means while S and $\dot{S}$ are Positive Big, the trajectory is far away from sliding plane, so we must use the Positive Big control force to make the system as soon as approach to sliding plane.

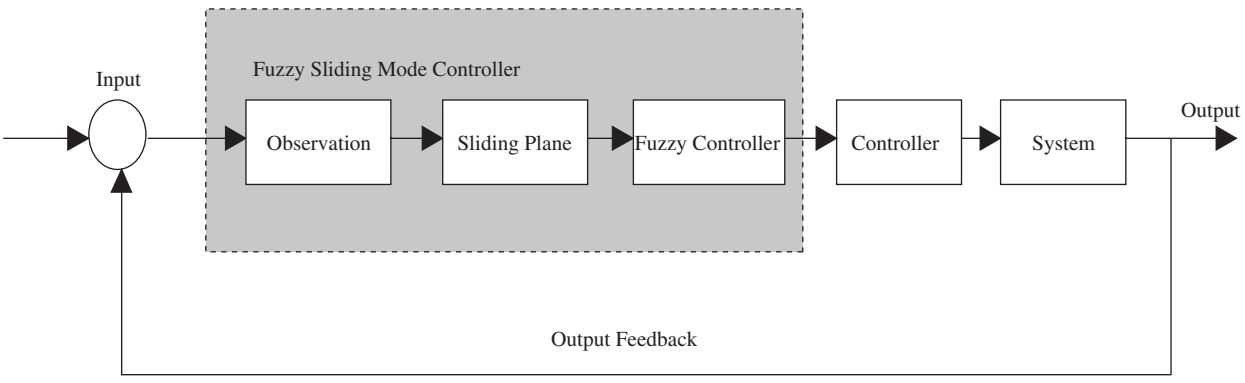

Fig. 2. Block diagram of fuzzy sliding mode control.

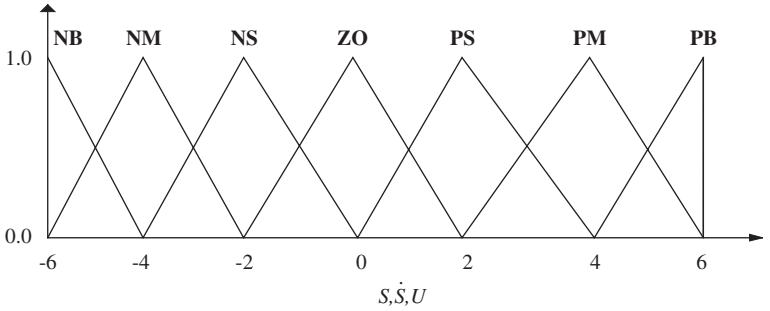

Fig. 3. The triangle membership functions of S, $\dot{S}$ and U.

Table 1
Linguistic rules of S and $\dot{S}$

		$\dot{S}$						
		NB	NM	NS	ZO	PS	PM	PB
S	NB	NB		NM		NS		ZO
	NM		NM		NS		ZO	
	NS	NM		NS		ZO		PS
	ZO		NS		ZO		PS	
	PS	NS		ZO		PS		PM
	PM		ZO		PS		PM	
	PB	ZO		PS		PM		PB

Table 2
The look-up table

Look-up table U		$\dot{S}$						
		NB	NM	NS	ZO	PS	PM	PB
S	NB	−1.0	−0.8	−0.6	−0.4	−0.2	−0.1	0
	NM	−0.8	−0.6	−0.4	−0.2	−0.1	0	0.1
	NS	−0.6	−0.4	−0.2	−0.1	0	0.1	0.2
	ZO	−0.4	−0.2	−0.1	0	0.1	0.2	0.4
	PS	−0.2	−0.1	0	0.1	0.2	0.4	0.6
	PM	−0.1	0	0.1	0.2	0.4	0.6	0.8
	PB	0	0.1	0.2	0.4	0.6	0.8	1.0

Rule 2: If S is PS and $\dot{S}$ is NS, then U is ZO. Its means while S is Positive Small and $\dot{S}$ is Negative Small, the trajectory is already in close to sliding plane and the reaching condition $S \cdot \dot{S} < 0$ is satisfied. It does not add the control force.

After setting up fuzzy linguistic control law and according to *Mamdani* inference method, we obtain the look-up Table as shown in Table 2. The values in Table 2 can be plotted as a control surface as shown in Fig. 4, in which U is a function of S and $\dot{S}$. The volume under a control surface is proportional to the amount of energy expended by the controller. Finally, the control force u of the system can be computed by $u = GU * U$, where GU is a constant which depends on the upper bound of $\mathbf{W}(\mathbf{Z}, t)$.

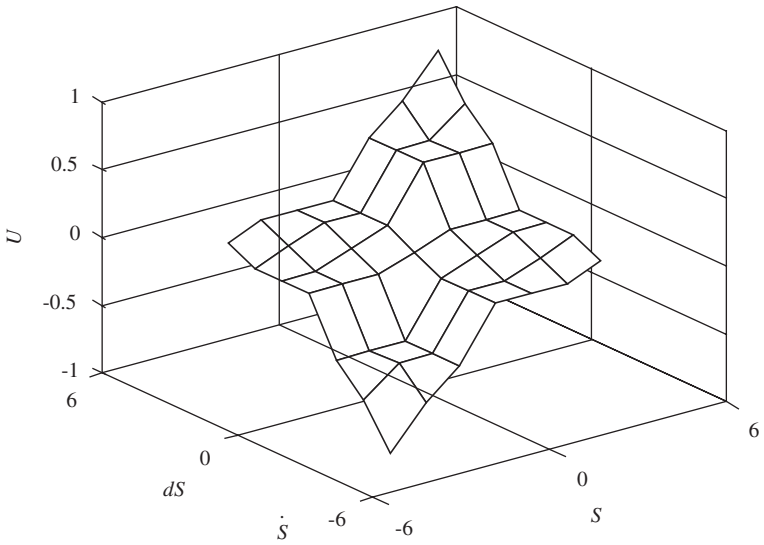

Fig. 4. Control surface for the FSMC.

4. Numerical results and discussion

4.1. The building model

Considering the building model is a distributed parameter beam system, one has the first-mode natural frequency [14]

$$\omega = \beta^2 \sqrt{\frac{EI}{\rho A}}. \tag{20}$$

In order to save the computational time, a three-slab RC building is selected as the example with the following parameters: total length $L = 9\,\text{m}$, Young's modulus $E = 2.1324 \times 10^2\,\text{N/m}^2$, cross-sectional area $0.075\,\text{m}^2$, mass density $7840\,\text{kg/m}^3$, mass of each slab is 777 kg, spring stiffness of ATMD is 6875.18 N/m, mass of ATMD is 125.94 kg, and the dry friction coefficient is 0.05. The dynamic responses of the system are solved by the *Runge–Kutta* method with the desired accuracy 10^{-6}. The initial shape is taken as the first mode shape [17] of free vibrations of a cantilever beam

$$v(x,0) = C_1\left[\sin\,\beta_1 x - \sinh\,\beta_1 x - \alpha_1(\cos\,\beta_1 x - \cosh\,\beta_1 x)\right], \tag{21}$$

where

$$\alpha_1 = \left(\frac{\sin\,\beta_1 l + \sinh\,\beta_1 l}{\cos\,\beta_1 l + \cosh\,\beta_1 l}\right), \quad \beta_1 l = 1.875104.$$

4.2. Numerical results and discussion

In numerical simulations, the performances of two control methods are compared with different initial conditions and the El Centro (1940), Kobe (1995) excitation earthquake.

In this study, the ratios of dynamic responses in the controlled and uncontrolled systems are used to judge the reduction of system responses. The $R(X_{\max})$ and $R(\dot{X}_{\max})$ are the ratios of maximum displacement and velocity of the controlled and uncontrolled systems, and are defined as, respectively,

$$R(X_{\max}) = (X_{\max})_{\text{controlled}}/(X_{\max})_{\text{uncontrolled}}, \tag{24a}$$

$$R(\dot{X}_{\max}) = (\dot{X}_{\max})_{\text{controlled}}/(\dot{X}_{\max})_{\text{uncontrolled}}, \tag{24b}$$

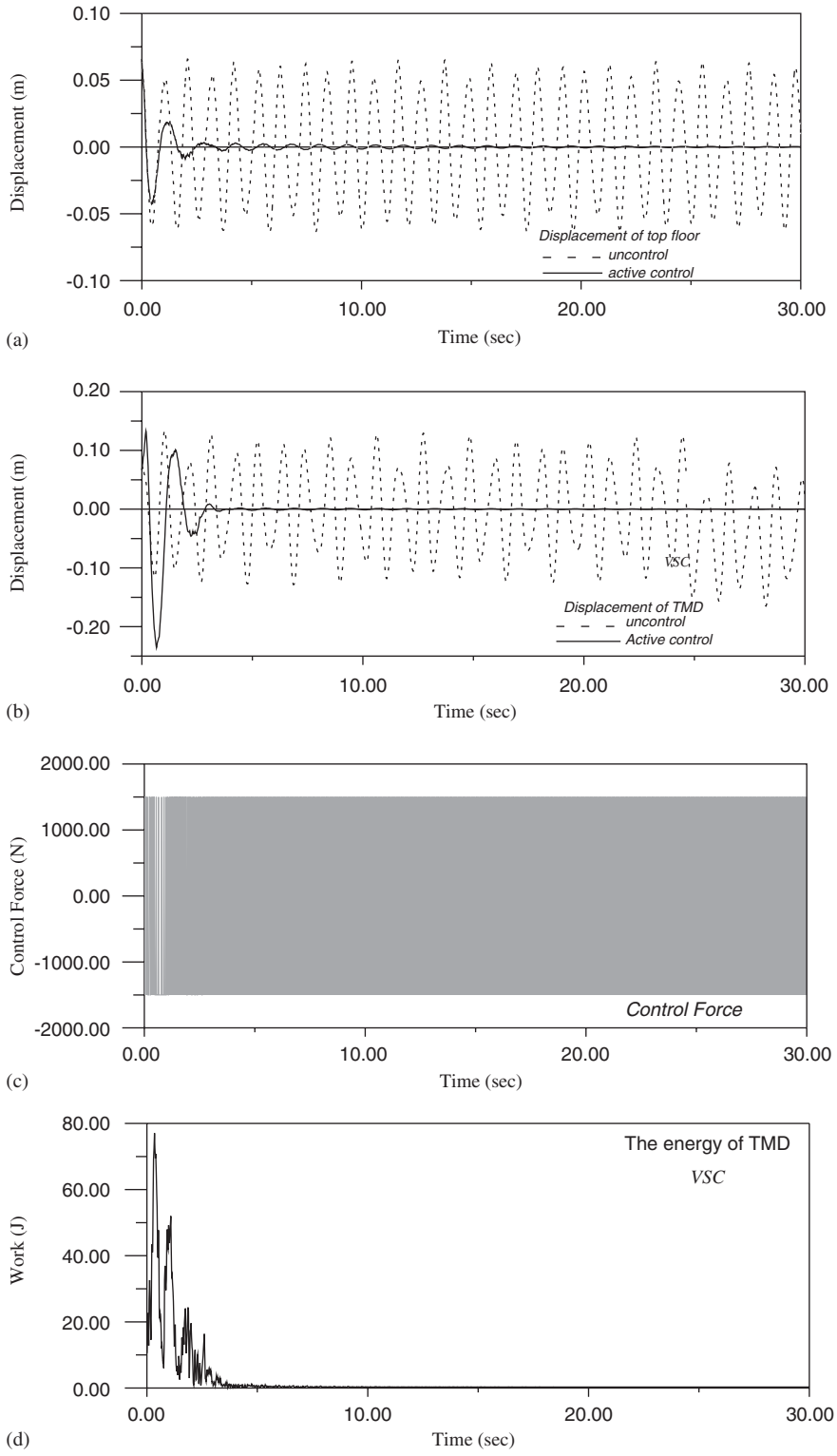

Fig. 5. Free vibrations (under external disturbance) of the uncontrolled and the VSC systems with nonzero initial condition: (a) displacement of top floor, (b) displacement of the TMD, (c) control force and (d) work done by the control force.

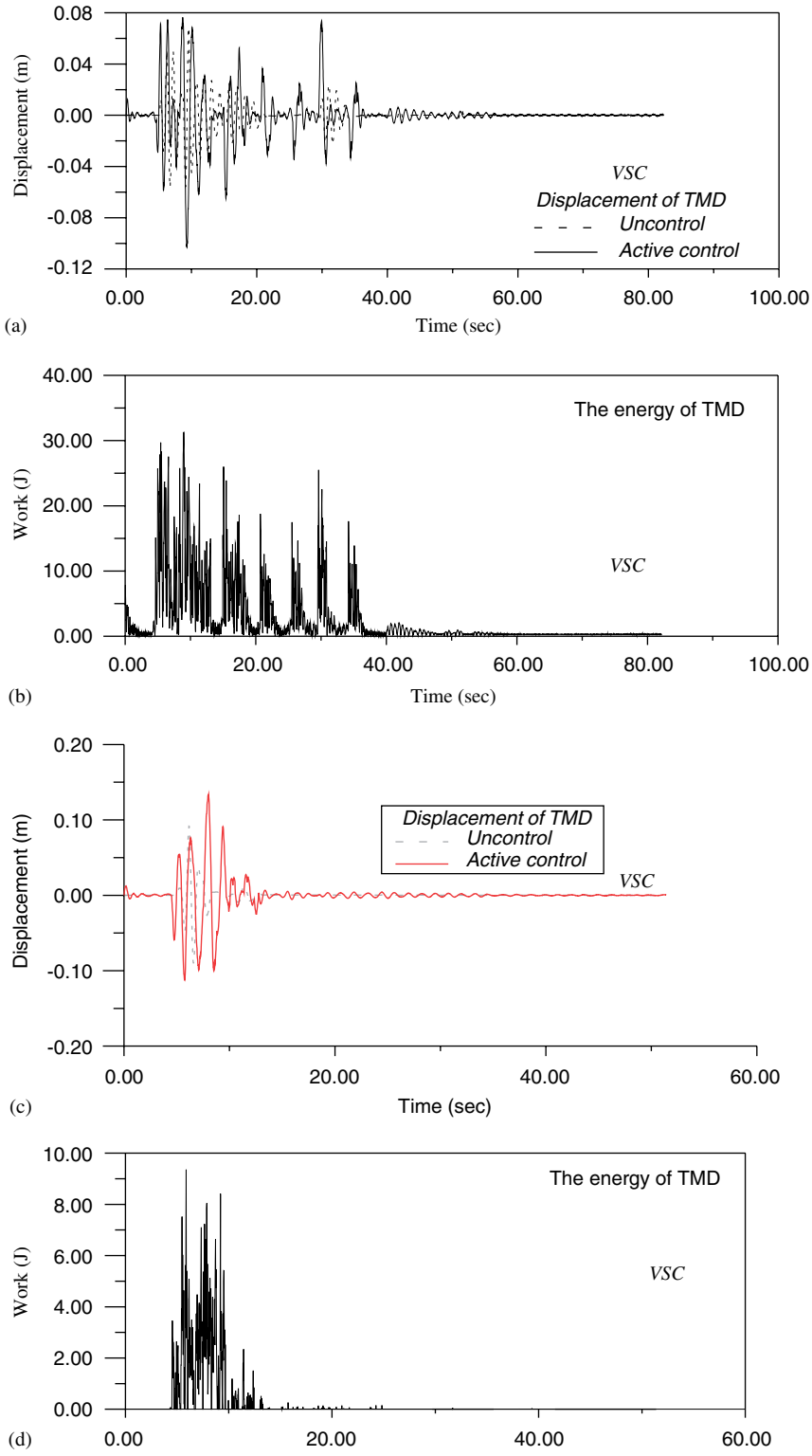

Fig. 6. Free vibrations (under external disturbance) of the uncontrolled and the VSC systems excited by the El Centro earthquake: (a) displacement of the TMD, (b) work done by the control force, the VSC systems excited by the Kobe earthquake, (c) displacement of the TMD and (d) work done by the control force.

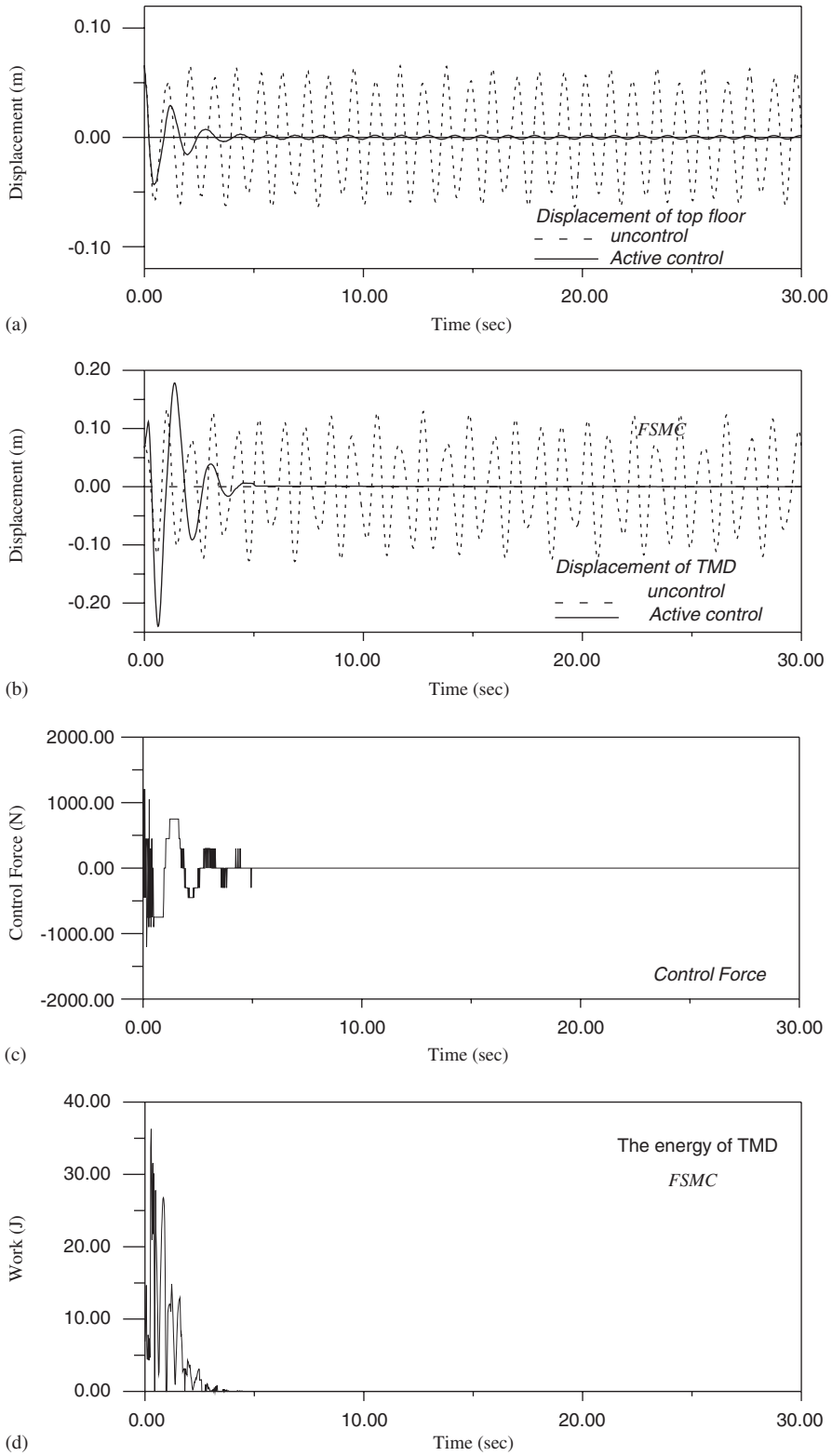

Fig. 7. Free vibrations (under external disturbance) of the uncontrolled and the FSMC systems with nonzero initial condition: (a) displacement of top floor, (b) displacement of the TMD, (c) control force and (d) work done by the control force.

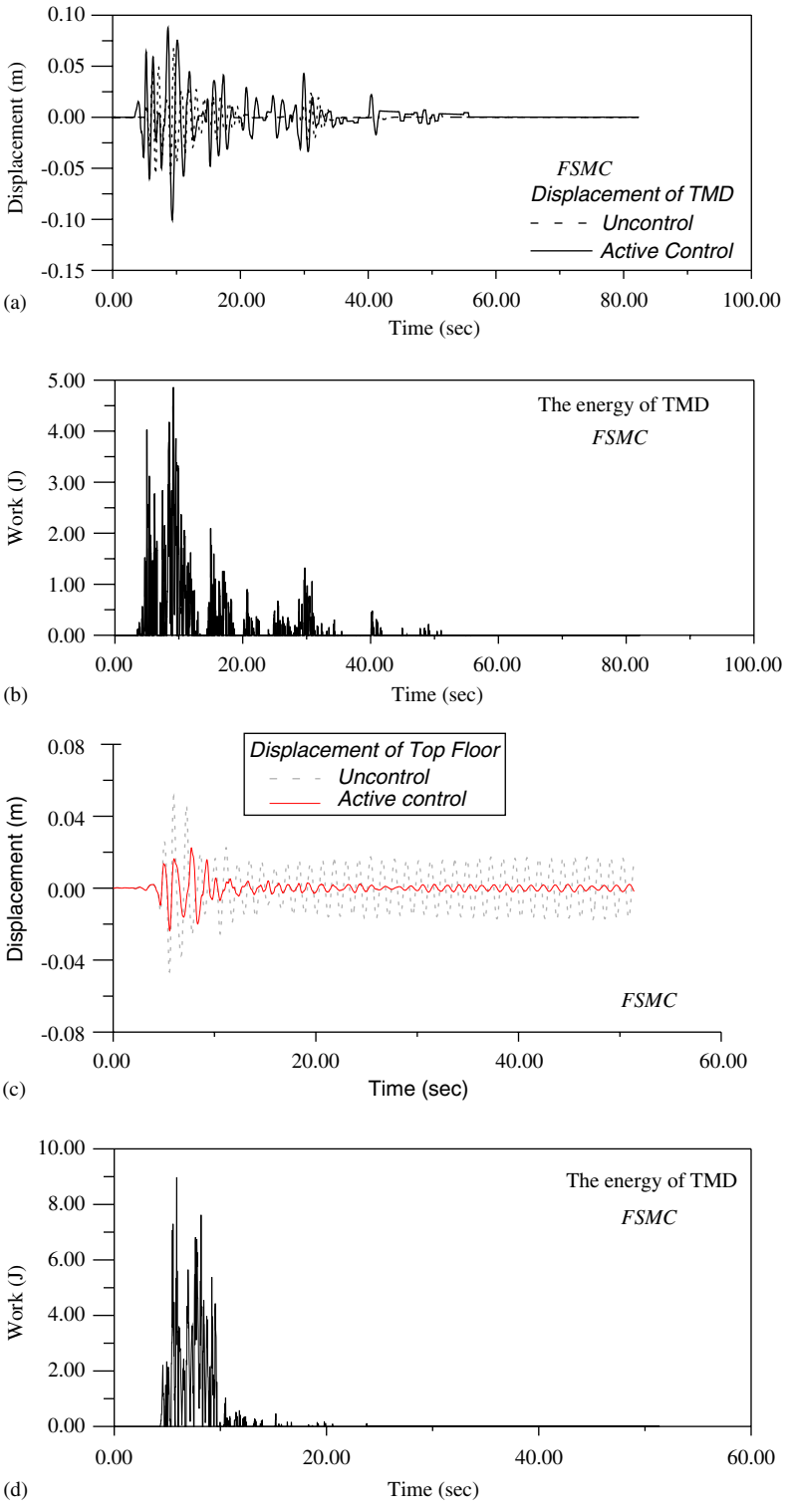

Fig. 8. Free vibrations (under external disturbance) of the uncontrolled and the FSMC systems excited by the El Centro earthquake: (a) displacement of the TMD, (b) work done by the control force, the FSMC systems excited by the Kobe earthquake, (c) displacement of the TMD and (d) work done by the control force.

The $R(X_{ave})$ and $R(\dot{X}_{ave})$ are the ratios for the average displacement and velocity of the controlled and uncontrolled systems during time interval T, and are defined as, respectively,

$$R(X_{ave}) = (X_{ave})_{controlled}/(X_{ave})_{uncontrolled},$$
$$R(\dot{X}_{ave}) = (\dot{X}_{ave})_{controlled}/(\dot{X}_{ave})_{uncontrolled}.$$

Fig. 5 shows the responses of the building system with an initial condition $C_1 = 0.0667$ in Eq. (21). The dash lines are used for the vibrations under external disturbance while the solid line represents the VSC system. Fig. 5(a, b) shows the displacement of top floor and TMD, respectively. Fig. 5(c) is the time history of control force, and Fig. 5(d) shows the decay of the work done by the control force and the settling time of the control response is about 3–4 s. Fig. 6 shows the displacements of the building subjected to the El Centro and Kobe earthquakes are controlled through the TMD. The responses of the TMD under the VSC control and without control are shown in Fig. 6(a) and (c), subjected to the El Centro and Kobe earthquakes, respectively. It shows that the VSC will greatly reduce the system response in comparison without control. Fig. 6(b) and (d) show the decay of the work done by the control force and the settling time of the control response is about 40 and 12 s subjected to the El Centro and Kobe earthquakes, respectively. The responses of the FSMC system are illustrated in Figs. 7 and 8. In the FSMC system, the membership function, language and the look-up table are calculated off line, but the observation and control force $u(t)$ are operated on line. Under the same initial condition as shown in Fig. 7, it is noticed that the FSMC has similar effect with the VSC, but the energy of control force is smaller than that of the VSC, because the control force of the VSC is similar to Bang-Bang control. Under the earthquakes of El Centro and Kobe excitation as shown in Fig. 8, the FSMC successfully suppresses the responses as same as the VSC, but the control energy is less than that of the VSC.

Comparisons of simulated responses of the VSC and the FSMC under the El Centro earthquake are shown in Table 3. It is found:

1. Comparing the maximum displacements of the top floor for the VSC and the FSMC with that of the uncontrolled system, it can be obtained $R(X_{max}) = 0.39$, and $R(X_{max}) = 0.167$, respectively. It is the reducible degrees of displacements are 61% and 83%, respectively. It is shown that the VSC and the FSMC control methods are all effective in reducing the displacements of the building structure.
2. Comparing the peak velocities of the top floor for the VSC and the FSMC with that of the uncontrolled system, the reducible degrees of velocity are 15% and 83%, respectively. It is shown that the FSMC control methods are more effective than that of the VSC in reducing the velocity of the building structure.
3. The root-mean-square (rms) of control energy of the FSMC is smaller than that of the VSC. The work done by the FSMC control force is smaller.

Table 3
Comparing performances for the VSC and the FSMC

El centro earthquake	X_{max} (m)	$\dot{X}_{max}$ (m/s)	X_{ave} (m)	$\dot{X}_{ave}$ (m/s)	$R(X_{max})$	$R(\dot{X}_{max})$	$R(X_{ave})$	$R(\dot{X}_{ave})$	U_{ave} (N)
Uncontrol	0.049	0.261	0.012	0.062					
VSC									
X_S	0.019	0.222	0.002	0.056	0.390	0.851	0.209	0.901	1500
X_T	0.103	0.727	0.007	0.181					
FSMC									
X_S	0.017	0.133	0.002	0.011	0.167	0.170	0.351	0.510	315.16
X_T	0.101	0.505	0.008	0.034					

5. Conclusions

In this paper, the VSC and the FSMC algorithms for structural building with TMD system has been developed. In the numerical simulations using the El Centro earthquake, it is shown that proposed control methods are all effective in reducing the responses of displacement and velocity of the building structure. The FSMC control methods are more effective than that of the VSC in reducing the velocity of the building structure. It is also found that the FSMC method has the smaller rms of control force than that of the VSC method. The performance of the FSMC is better than the SMC.

Appendix A

A.1. Kinetic and strain energies

The total kinetic energy of the whole system is

$$T_m = \frac{1}{2} M_G[\dot{b} + \dot{v}(L,t) + \dot{\xi}]^2 + \frac{1}{2}\rho A \int_0^L (\dot{v} + \dot{b})^2 \,\mathrm{d}x + \frac{1}{2}\sum_{i=1}^{n} m_i[\dot{v}(x_i,t) + \dot{b}]^2, \tag{A.1}$$

where the first term is kinetic energy of the TMD, the second term is for the building being modeled by the beam theory, and the last one is for the floors.

Assuming that the beam is inextensible, the axial tension due to gravity is

$$G(x) = g\left[\sum_{i=1}^{n} m_i H(x_i - x) + \rho A(L - x) + M_G\right], \tag{A.2}$$

where H is the unit step function. The strain energy of the beam can be written as

$$U_m = \frac{1}{2}\int_0^L \left[G(x)v_x^2 + EIv_{xx}^2 + \frac{1}{4}EAv_x^4\right]\mathrm{d}x, \tag{A.3}$$

where the geometric nonlinearity is considered.

A.2. Virtual work

From the free-body diagram shown in Fig. 1(c), the virtual work done by the applied forces acting on the TMD may be written in terms of its virtual displacement $\delta\xi$ as

$$\delta W = [F - k\xi - \mu M_G g\,\mathrm{sgn}(\dot{\xi})]\delta\xi. \tag{A.4}$$

A.3. Finite element discretization

By using the finite element method, the continuous displacements may be approximated in terms of the discretized nodal displacement [15,16]. In this paper, the beam is divided into n elements and each node has two degrees-of-freedom. The usual approach in the finite element method is that each unknown deformation $v(x,t)$ is approximated by a finite series in the following form:

$$v(x,t) = \sum_{i=1}^{n} \mathbf{H}_i(x) q_i(t), \tag{A.5}$$

where $\mathbf{H}_i(x)$ is the *Hermite* shape function [15] and $\mathbf{q}_i(t)$ represents the nodal displacement.

A.4. The governing equation

By using *Hamilton's* principle

$$\int_{t_1}^{t_2} \sum_{j=1}^{N_e} \delta L_j \, \mathrm{d}t + \delta W = 0, \tag{A.6}$$

we obtain a set of nonlinear, second-order ordinary differential equations

$$\mathbf{M}\ddot{\mathbf{Q}} + \mathbf{K}\mathbf{Q} + \mathbf{N}(\mathbf{Q}) = \mathbf{P}, \tag{A.7}$$

where $\mathbf{M}$ and $\mathbf{K}$ are the global mass and stiffness matrices, $\mathbf{N}(\mathbf{Q})$ represents the nonlinear term, and $\mathbf{P}$ is the force vector. The dynamic formulation can be seen in the Appendix. It should be noted that the force vector $\mathbf{P}$ includes the acceleration $\ddot{b}$ of earthquake, actuating force F and dry friction force $\mu M_G g \,\mathrm{sgn}(\dot{\xi})$.

To compensate for the dissipation mechanisms, it is customary to use the most popular hypotheses known as the *Rayleigh damping*:

$$\mathbf{C} = \alpha\mathbf{M} + \beta\mathbf{K}, \tag{A.8}$$

where the coefficients α and β are selected to fit the structure under consideration.

Finally, we obtain the equation of motion for the damped system

$$\mathbf{M}\ddot{\mathbf{Q}} + \mathbf{C}\dot{\mathbf{Q}} + \mathbf{K}\mathbf{Q} + \mathbf{N}(\mathbf{Q}) = \mathbf{P}. \tag{A.9}$$

A.5. Hamilon's principle

For each element, the displacements at each nodal point are assumed to be composed of the transverse deformation v and its slope v_x. The *Hermite* shape function [16,17] is defined to satisfy continuity requirements of the displacement nodal value and slope. Each of the shape functions is of cubic polynomial and is represented by

$$H_i = a_i + b_i\eta + c_i\eta^2 + d_i\eta^3, \quad -1 \leqslant \eta \leqslant 1, \quad i = 1, 2, 3, 4. \tag{A.10}$$

When all conditions are satisfied, the coefficients, a_i, b_i, c_i, d_i, can be easily obtained.

By using Eqs. (A.5) and (A.10), the kinetic and strain energies for an element associated with the TMD can be obtained, respectively, as

$$\begin{aligned} T_j &= \frac{1}{2}\int_{x_j}^{x_{j+1}} \{\rho A(\mathbf{H}\dot{\mathbf{q}} + \dot{b})^{\mathrm{T}}(\mathbf{H}\dot{\mathbf{q}} + \dot{b}) + m_j(\mathbf{H}_j\dot{\mathbf{q}} + \dot{b})^{\mathrm{T}}(\mathbf{H}_j\dot{\mathbf{q}} + \dot{b}) + M_G(\mathbf{H}_L\dot{\mathbf{q}} + \dot{b} + \dot{\xi})^{\mathrm{T}}(\mathbf{H}_L\dot{\mathbf{q}} + \dot{b} + \dot{\xi})\}\mathrm{d}x, \\ U_j &= \frac{1}{2}\int_{x_j}^{x_{j+1}} \{G(x)(\mathbf{B}\mathbf{q})^{\mathrm{T}}(\mathbf{B}\mathbf{q}) + EI(\mathbf{D}\mathbf{q})^{\mathrm{T}}(\mathbf{D}\mathbf{q}) + \frac{1}{4}EA(\mathbf{B}\mathbf{q})^{\mathrm{T}}(\mathbf{B}\mathbf{q})(\mathbf{B}\mathbf{q})^{T}(\mathbf{B}\mathbf{q})\}\mathrm{d}x - \frac{1}{2}k\xi^2, \end{aligned} \tag{A.11}$$

where $\mathbf{B} = (\mathrm{d}/\mathrm{d}x)\mathbf{H}$, $\mathbf{D} = (\mathrm{d}^2/\mathrm{d}x^2)\mathbf{H}$, and $\mathbf{H}_L$ represents the $\mathbf{H}$ at $x = \ell$.

After some manipulations in Hamilton's principle (A.6), we can obtain the motion Eq. (A.9) with the following matrices:

$$\mathbf{Q} = \begin{bmatrix} q_1 & \cdots & q_i & \cdots & q_{2N_e} & \xi \end{bmatrix}^{\mathrm{T}},$$

$$\mathbf{M} = \begin{bmatrix} & & & & 0 & \\ & & & & \vdots & \\ & & \mathbf{M}^* & & M_G & \\ & & & & 0 & \\ 0 & \cdots & M_G & 0 & M_G & \end{bmatrix}_{(2N_e+1)\times(2N_e+1)},$$

$$\mathbf{K}=\begin{bmatrix} & & & 0\\ & & & \vdots\\ & \mathbf{K}^* & & -k\\ & & & 0\\ 0 & \dots & 0 \quad 0 & k \end{bmatrix}_{(2N_e+1)\times(2N_e+1)},$$

$$\mathbf{P}=\begin{Bmatrix} \rho A\ddot{b}+m\ddot{b}\\ \rho A\ddot{b}\\ \rho A\ddot{b}+m\ddot{b}\\ \vdots\\ \rho A\ddot{b}+m\ddot{b}+M_G\ddot{b}\\ \rho A\ddot{b}\\ M_G\ddot{b}-F+\mu M_G\mathrm{sgn}(\dot{\xi}) \end{Bmatrix}_{(2N_e+1)\times 1}, \quad \mathbf{N}(\mathbf{Q})=\frac{1}{2}EA\mathbf{B}^{\mathrm{T}}\mathbf{B}\mathbf{q}\mathbf{q}^{\mathrm{T}}\mathbf{B}^{\mathrm{T}}\mathbf{B}, \tag{A.12}$$

$$\mathbf{M}^*=\sum_{j=1}^{N_e}(\rho A\mathbf{N}^{\mathrm{T}}\mathbf{N}+m_j\mathbf{N}_j^{\mathrm{T}}\mathbf{N}_j)=\begin{bmatrix} M_{11} & & & & \mathbf{O}\\ & M_{22} & & & \\ & & \ddots & & \\ & & & M_{(n-2)(n-2)} & \\ \mathbf{O} & & & & M_{(n-1)(n-1)} \end{bmatrix}.$$

$$\mathbf{K}^*=\sum_{j=1}^{N_e}[G(x)\mathbf{B}^{\mathrm{T}}\mathbf{B}+EI\mathbf{D}^{\mathrm{T}}\mathbf{D}].$$

A.6. The coefficients of the state-space equation

The coefficients of the state-space Eq. (A.4) are

$$\mathbf{Z}=\begin{bmatrix}\mathbf{Q}\\ \dot{\mathbf{Q}}\end{bmatrix}, \quad \mathbf{A}=\begin{bmatrix}\mathbf{O}_n & \mathbf{I}_n\\ -\mathbf{M}^{-1}\mathbf{K} & -\mathbf{M}^{-1}\mathbf{C}\end{bmatrix}, \quad \mathbf{B}=\begin{bmatrix}\mathbf{O}_{2n-3}\\ \mathbf{K}_1\mathbf{K}_2^{-1}\\ 0\\ -\mathbf{K}_2^{-1}\end{bmatrix},$$

$$\mathbf{W}=\begin{bmatrix}\mathbf{O}_n\\ \mathbf{W}_1(\ddot{b},t)\end{bmatrix}+\begin{bmatrix}\mathbf{O}_n\\ \mathbf{W}_2(\dot{\xi},t)\end{bmatrix}+\begin{bmatrix}\mathbf{O}_n\\ \mathbf{W}_3(\mathbf{Q},t)\end{bmatrix}, \tag{A.13}$$

in which

$$\mathbf{K}_1=\mathbf{M}_{(n-2)(n-2)}^{-1}\mathbf{M}_G, \quad \mathbf{K}_2=\mathbf{M}_G(1-\mathbf{K}_1),$$

$$\mathbf{W}_1(\ddot{b},t)=\mathbf{M}^{-1}\begin{bmatrix}\rho A\ddot{b}+m\ddot{b}\\ \rho A\ddot{b}\\ \rho A\ddot{b}+m\ddot{b}\\ \vdots\\ \rho A\ddot{b}+m\ddot{b}+M_G\ddot{b}\\ \rho A\ddot{b}\\ M_G\ddot{b}\end{bmatrix},\quad W_2(\dot{\xi},t)=\begin{bmatrix}\mathbf{O}_{n-1}\\ \mu M_G g\,\mathrm{sgn}(\dot{\xi})\end{bmatrix},$$

$$\mathbf{W}_3(\mathbf{Q},t)=-\mathbf{M}^{-1}\mathbf{N}(\mathbf{Q}). \tag{A.14}$$

$\mathbf{O}_n$ is a zero matrix $(n\times n)$ and $\mathbf{I}_n$ is an identity matrix $(n\times n)$. In Eq. (A.5), $\mathbf{W}_1(\ddot{b},t)$ is used for the earthquake excitation, $\mathbf{W}_2(\dot{\xi},t)$ represents the dry friction forces, and $\mathbf{W}_3(\mathbf{Q},t)$ is the nonlinear term.

References

[1] R.J. Mcnamara, Tuned mass dampers for buildings, *Journal of the Structure Division, ASCE* 103 (1977) 1785–1798.

[2] J.R. Sladek, R.E. Klingner, Effect of tuned mass dampers on seismic response, *Journal Structure Engineering, ASCE* 109 (1983) 2004–2009.

[3] J.T.P. Yao, Concept of structural control, *Journal of the Structure Division, ASCE* 98 (ST7) (1972) 1567–1574.

[4] V.I. Utkin, *Sliding Modes and their Application in Variable Structure system*, MIR Publishers, Moscow, 1974 (1978 English Translation).

[5] R.A. DeCarlo, S.H. Zak, G.P. Matthnews, Variable structure control of nonlinear multivariable system: a tutorial, *IEEE* 76 (1988) 212–232.

[6] L.A. Zadeh, Fuzzy set, *Information and Control* 8 (1965) 338–353.

[7] E.H. Mamdani, Application of fuzzy algorithms for control of simple dynamic plants, *IEE* 121 (12) (1974) 1585–1588.

[8] C.B. Brown, J.T.P. Yao, Fuzzy sets and structural engineering, *Journal of the Structure Division, ASCE* 109 (1983) 1211–1225.

[9] C. Juang, D.J. Elton, Fuzzy logic for estimation of earthquake intensity based on building damage records, *Civil Engineering System* 3 (1986) 187–191.

[10] G.C. Hwang, A.P. Wang, S.C. Lin, Application of fuzzy sliding mode control to pneumatic servo system, *Proceedings of the National Science Council Part A: Taiwan* 16 (1993) 340–346.

[11] S. Ankireddi, H.T.Y. Yang, Simple ATMD control methodology for buildings subject to wind loads, *Journal of the Structure Division, ASCE* 122 (1996) 83–91.

[12] C.H. Loh, C.H. Chao, Effectiveness of active tuned mass damper and seismic isolation on vibration control of multi-story building, *Journal of Sound and Vibration* 193 (4) (1996) 773–792.

[13] L.E. Mackriell, K.C.S. Kwok, B. Samali, Critical mode control of a wind-loaded building using an active tuned mass damper, *Engineering Structures* 19 (1997) 834–842.

[14] A.P. Wang, R.F. Fung, S.C. Huang, Dynamic analysis of a tall building with a tuned-mass-damper device subjected to earthquake excitation, *Journal of Sound and Vibration* 244 (1) (2001).

[15] C.C. Spyrakos, *Finite Element Modeling in Engineering Practice*, West Virginia University Press, West Virginia, 1994.

[16] P.H. Wang, R.F. Fung, M.J. Lee, Finite element analysis of a three-dimensional underwater cable with time-dependent length, *Journal Sound and Vibration* 209 (2) (1998) 223–249.

[17] S.S. Rao, *Mechanical Vibration*, third ed., Addison-Wesley, Cambridge, MA, 1995.